Journal of Energy Storage 88 (2024) 111601

Contents lists available at ScienceDirect

Journal of Energy Storage

journal homepage: www.elsevier.com/locate/est

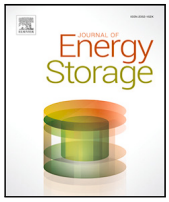

Research papers

Optimal operation of pumped storage power plants with fixed- and variable-speed generators in multiple electricity markets considering overload operation

Domagoj-Krešimir Jukić [a,*], Andreas Kugi [b,a], Wolfgang Kemmetmüller [a]

[a] Automation and Control Institute, TU Wien, Vienna, Austria
[b] Austrian Institute of Technology (AIT), Vienna, Austria

ARTICLE INFO

Keywords:
Optimal operation
Pumped storage power plant
Day-ahead market
Intraday market
Ancillary services
Bidding curve generation

ABSTRACT

This work studies the optimal operation of pumped storage power plants with fixed- and variable-speed generators in different electricity markets. This paper extends the state of the art by systematically considering the detailed plant behavior for heterogeneous pumped storage power plants and the possible short-term electrical overload operation. The Day-Ahead, ancillary service, and Intraday markets are studied in the first part by developing a mixed integer nonlinear problem (MINLP). The results demonstrate that variable-speed units, especially if equipped with doubly-fed induction machines (DFIMs), yield the highest profit, particularly in the presence of automatic Frequency Restoration Reserve (aFRR). The proposed optimization of the Intraday market shows that the total profit of the Day-Ahead, Ancillary services, and Intraday markets are the highest in the case of variable-speed units with aFRR, where it might be a drawback offering Frequency Containment Reserve. Finally, a robust optimization-based bidding curve generation strategy is developed in the last step. The strategy allows the plant to operate with high profits under price prediction uncertainties and enables optimal reservoir management. The developed optimization tasks and the bidding curve generation strategy also exhibit shorter computation times than the state-of-the-art strategies.

1. Introduction

New installations of renewable energy sources (RES) increased by 17% in 2021 due to the consecutive increase in investments. This resulted in 175 GW of new additions of solar photovoltaic power and 102 GW of wind power globally. In the same year, solar and wind power provided for the first time more than 10% of the world's electricity [1]. The power system operation is changing despite the relatively small share of solar and wind power, mainly due to their intermittent nature. This requires a high ramping capability of the power system to follow the net load variations [2,3] and an increase in balancing services and reserves for frequency control [4]. Another challenge in the power system operation with a high share of intermittent RES is the curtailment problem in the case of an excess of supply when conventional generators cannot reduce their output due to technical constraints [4]. Pumped storage power plants (PSPPs) present a proven technology to mitigate these effects. They can efficiently store energy at a large scale and provide ancillary services [4–6].

PSPPs were traditionally operated to satisfy the load utilizing hydro-thermal coordination [4]. In the liberalization process of electricity markets, they continued their operation by utilizing the energy arbitrage on the Day-Ahead market – using the price difference in the electricity market by storing energy during low prices (off-peak hours) and producing power from the stored energy during high prices (peak hours) [4,7,8]. This operational mode requires a high price difference to be profitable and to recover the PSPP investment costs. However, the works [9,10] showed that a rising penetration level of RES leads to lower average electricity prices and a lower price difference between peak and off-peak hours, resulting in a flattened price profile. In order to increase profit, PSPPs are additionally participating in ancillary service markets [4,11,12] and Intraday markets [13]. The automatic Frequency Restoration Reserve (aFRR) is here a major source of income [5,14] and the Frequency Containment Reserve (FCR) might be an additional source of income [15]. Units providing these additional services must be connected to the grid to meet the requested activation times [16]. Additionally, the provision of FCR and/or aFRR changes the units' output power and operating point. Thus, high flexibility of the PSPP is required. Units with synchronous generators (SGs) do not allow for this flexibility due to their fixed speed. They have a

* Corresponding author.
E-mail addresses: Jukic@acin.tuwien.ac.at (D.-K. Jukić), kugi@acin.tuwien.ac.at (A. Kugi), kemmetmueller@acin.tuwien.ac.at (W. Kemmetmüller).

https://doi.org/10.1016/j.est.2024.111601
Received 12 January 2024; Received in revised form 9 March 2024; Accepted 3 April 2024
Available online 12 April 2024

high efficiency only in a narrow band near the rated power, which is especially visible in the pump mode [17]. Thus, fixed-speed units can provide ancillary services only in the turbine mode. A hydraulic short-circuit can be used to provide ancillary services also in the pump mode [4]. Another possibility is to use variable-speed units, which are equipped with doubly-fed induction machines (DFIMs) or converter-fed synchronous generators (CFSGs), as they have increased flexibility in the form of high efficiency over an extended operating range, and they also allow for power control in the pump mode. The main drawback of variable-speed generators is the slightly reduced efficiency at higher powers due to the additional converter losses [17] and the increased investment costs [18]. However, variable-speed technology is very promising [19,20].

PSPPs are limited by a series of operational constraints. The primary limit is the power range of the units. The reduced efficiency and the increased cavitation and wear of Francis pump–turbines limit the minimum power. The maximum power is given by the maximum producible power and the generator nameplate power, which is determined by thermal constraints. Additional constraints include the feasible water head and outflow of the reservoirs. All these effects must be taken into account in order to operate the PSPP optimally. Additionally, the characteristics of the different unit types need to be considered. This requires a mathematical model tailored to the optimization task. A detailed nonlinear model of the PSPP can be developed with the available plant data, see, e.g., [17,21,22]. However, such nonlinear models result in a nonlinear programming (NLP) problem that is difficult to solve. The complexity additionally increases as the power range between zero and minimum power in the turbine and pump mode is not feasible, resulting in a non-convex optimization set. This can be circumvented by transforming the optimization problem into a mixed integer (MI) problem by introducing status bits, leading to a MINLP. The solution methods for MINLPs have yet to reach the maturity of linear programming (LP) problems or NLPs, making them often not applicable [23]. This problem can be solved by: (i) using a linear model which results in a MILP, see [3,5,8,19,20,24–28], (ii) neglecting constraints and transforming the problem to an NLP, see [23,29–31], or (iii) using a linear model and neglecting constraints and transforming the problem into an LP, see [2,12,28–32]. These simplifications allow us to formulate an optimization problem that can be solved in the required fast calculation times. However, they are not always justified. For instance, neglecting the head variation can introduce significant model errors if the head variation is large [23]. The work [33] circumvents this problem by solving the exact NLP in the first stage and an approximate LP in second stage. Nevertheless, this work also does not consider all important effects, e.g., the power influence on the efficiency. The authors are not aware of any work developing a detailed PSPP model tailored to energy market optimizations. This is, in particular, true for heterogeneous plants, i.e., plants where different (fixed- and variable-speed) generator types are combined.

The optimal operation of PSPPs in different markets is widely studied [34]. These studies range from optimizations of a single unit on the Day-Ahead market to optimizations of the full power plant on the Day-Ahead, ancillary services, and Intraday markets [4]. Additionally, PSPPs are often optimized in a portfolio of different plants, particularly in combination with wind power, see [12], or photovoltaic power, see [3], due to the complementing characteristics. Another trend is to investigate possibilities to increase the participation of PSPPs in ancillary service markets. The works [5,24,25] study the influence of the hydraulic short-circuit operation of fixed-speed units, showing that the total profit increases compared to conventional fixed-speed units. The reason is the increased operating range of the units, which results in higher participation and revenue from the aFRR market. The work [19] studies the impact of a generic variable-speed technology on the profit, and [20] compares the profit of DFIM and CFSG technologies. It is shown that the profit is higher with variable-speed units than with fixed-speed units due to the extended operating range. The results also show that the DFIM has higher profits than the CFSG due to the smaller converter losses. The hydraulic short-circuit of variable- and fixed-speed units was studied in [8]. As a result, variable-speed generators have a higher profit than fixed-speed generators with or without a hydraulic short-circuit operation. All mentioned works have in common that simplified plant models are used. However, comparing different generator technologies requires detailed models covering the whole operating range, which differs from the given literature.

Most previously given studies perform deterministic optimizations with a known price. However, the price of the electricity market is not accurately known in advance. Thus, the given methods can be employed for an a posteriori study of the plant for given price profiles, but they cannot be used to trade on electricity markets. To participate in the electricity market, plant operators need to submit supply and demand curves. These curves contain multiple sorted price–power pairs, which need to create non-decreasing curves, i.e., the bidding power needs to be non-decreasing for a price increase. Price forecasts are used to create supply and demand curves for price-taker plants [35]. These predictions range from the prediction of confidence intervals to the probability distribution prediction [36]. Depending on the available data, different methods, i.e., robust optimization, stochastic optimization, and Monte Carlo simulations [35,37–39] are applied to generate these curves. The work [37] developed a simple, robust optimization strategy for a thermal power plant unit, leading to a better performance than the bidding strategy from [40]. However, the bidding strategy from [37] only applies to plants without energy storage, as the proposed method can only be used to generate supply curves. These concepts are further extended in [35] to a robust optimization method for generating supply and demand curves for a generic energy storage facility. However, the additional constraints to ensure non-decreasing bidding curves require the optimization problems to be solved sequentially, which might not be feasible if applied to a PSPP within the required computation time.

This paper aims to contribute to the identified research gap by studying the optimal operation of a pumped storage power plant with fixed- and variable-speed units and heterogeneous plants in the European Power Exchange (EPEX SPOT) SE. A price-taker PSPP, i.e., a plant with negligible influence on the market-clearing price, is assumed here. The first contribution is the development of an accurate mathematical model for a PSPP tailored to the optimal trading on the electricity market. The developed model includes all essential effects, like the efficiency change with the piezometric pump–turbine head and the generator power, and the minimum and maximum power bounds, including the maximum producible unit powers. The model also includes a simplified thermal model of the generators to study the possible profit increase if the generators are (shortly) operated with an electrical overload but within the permissible temperature range. The second contribution is a study of the profits of different generator types in the Day-Ahead market with and without ancillary services (FCR and aFRR). The SG, CFSG, and DFIM are studied here, where detailed generator characteristics are considered. Another important contribution is the study of additional profits in the continuous Intraday market. These profits are based on the unused power reserves of the ancillary services and the Intraday market's high price volatility. The last contribution of this work is a strategy for bidding curve generation based on robust optimization.

The paper is organized as follows: The mathematical model, which forms the basis for the optimal short-term operation of the PSPP, is described in Section 2. The Day-Ahead market with and without ancillary services is studied in Section 3, and the continuous Intraday market is analyzed in Section 4. The bidding curve generation strategy for PSPPs is given in Section 5. Finally, Section 6 contains a short conclusion.

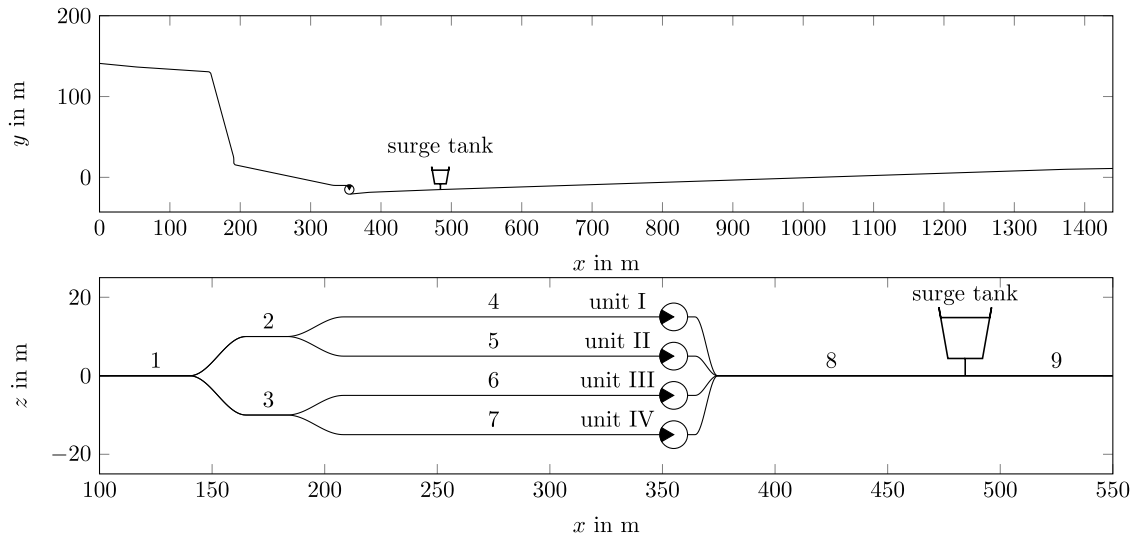

Fig. 1. Setup and spatial dimensions of the considered PSPP, including pipelines 1 to 9, units I to IV, and the downstream surge tank.

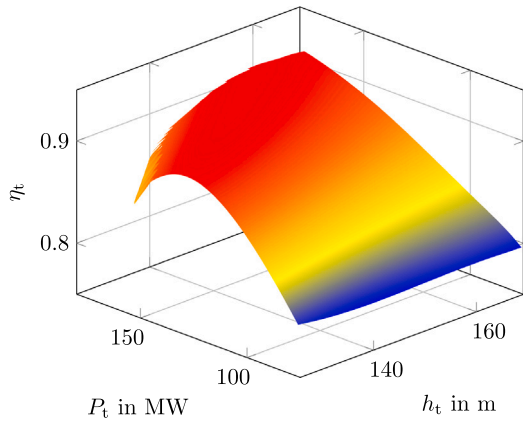

Fig. 2. Efficiency map of a plant unit with a Francis pump–turbine and a DFIM in turbine mode: efficiency η_t as a function of the electric power P_t and the piezometric head of the pump–turbine h_t.

2. Mathematical model

2.1. Plant

The considered plant is depicted in Fig. 1. The same plant was considered in the authors' previous papers [17,41], where a detailed dynamical model was developed, which, e.g., covers the pressure waves within the pipelines. This model is high-dimensional and thus unsuitable for (short-term) PSPP optimization in the electricity market. However, this model will be used to develop an accurate yet low-dimensional model suited for optimal dispatch problems. The basis is the stationary optimization given in [17], which calculates the optimal operating points of every plant unit (Francis pump–turbine and generator) at different desired plant powers and pump–turbine heads, see Fig. 2.

The efficiency of every unit at the optimal operating point is then used to develop unit efficiency maps, which are approximated by a sum of Gaussian functions [21]. This approximation allows us to analytically obtain the gradients of the efficiency maps with respect to their arguments, which is beneficial for optimization problems [22]. A significant benefit of the proposed approach is that these efficiency maps already include all operational limits of the pump–turbine and different generator types, as all of them are considered in the detailed model used for the stationary optimization. The detailed model was also verified, and the developed efficiency maps accurately describe the considered units, see [17,41].

The approximated maps are used to calculate the volumetric flow q of every unit for a given electrical unit power P. The model for every unit m, $m = 1, \dots, M$, with the total number of units $M = 4$, is given by

$$q_{t,m} = \frac{P_{t,m} s_{t,m}}{\rho g h_{t,m} \eta_{t,m}(P_{t,m}, h_{t,m})} \tag{1a}$$

$$q_{p,m} = \frac{P_{p,m} s_{p,m} \eta_{p,m}(P_{p,m}, h_{t,m})}{\rho g h_{t,m}}, \tag{1b}$$

with the powers in the turbine and pump mode $P_{t,m}$ and $P_{p,m}$, respectively, the status bits $s_{t,m}$ and $s_{p,m}$, the pump–turbine head $h_{t,m}$, the water density ρ and gravitational acceleration g. Here, $\eta_{t,m}$ and $\eta_{p,m}$ are the evaluated efficiencies in the turbine and pump mode, respectively. The status bits are used to consider the units' status, that is, if it is running ($s = 1$) or at a standstill ($s = 0$). The overall unit volumetric flow is given by $q_m = q_{t,m} - q_{p,m}$, and the total PSPP volumetric flow reads as $q_{pspp} = \sum_{m=1}^{M} q_m$.

The unit efficiency maps do not consider the head loss in the pipeline system. Thus, the additional head loss Δh_i of every pipeline i is modeled using a concentrated parameter resistance R_i by

$$\Delta h_i = R_i q_i |q_i|, \tag{2}$$

with the volumetric pipeline flow q_i. The pump–turbine head $h_{t,m}$ of unit m is thus given by

$$h_{t,m} = h_g - \sum_{i \in \mathcal{I}_m} \Delta h_i, \tag{3}$$

with the gross head h_g, and the set of all pipelines between the pump–turbine m and the reservoirs $\mathcal{I}_m$. The gross head h_g is modeled by the mass balance as

$$\frac{\mathrm{d}h_g}{\mathrm{d}t} = \frac{-q_{pspp}}{A_r}, \tag{4}$$

with the cross-sectional area of the reservoir A_r.

2.2. Thermal system

The generators' power and current limits are defined by the thermal limits of the machine in continuous operation. Therefore, safe operation with a power higher than the nominal power is allowed as long as the machine temperature remains in the feasible region. Otherwise, a

significant reduction of the winding insulation and generator lifetime occurs [42]. A thermal model of the generators is needed to study the possible benefits of a generator overload. Thermal machine models are usually high order [42] and are unsuitable for optimal dispatch calculations for PSPPs. Measurement data of a real plant showed that the critical winding temperature $T_{\mathrm{w},m}$ can be approximated with sufficient accuracy by the model

$$\frac{\mathrm{d}T_{\mathrm{w},m}}{\mathrm{d}t} = \left(a_{0,m} + a_{1,m}s_m\right) T_{\mathrm{w},m} + b_{0,m}S_m + \left(c_{0,m} + c_{1,m}s_m\right) T_{\mathrm{a}}. \tag{5}$$

$S_m = |P_m|/\cos(\varphi_m)$ is the apparent power of the unit m calculated over the provided active power $P_m = P_{\mathrm{t},m}s_{\mathrm{t},m} - P_{\mathrm{p},m}s_{\mathrm{p},m}$ and the power factor $\cos(\varphi_m) = 0.9$. Moreover, $s_m = s_{\mathrm{t},m} \vee s_{\mathrm{p},m}$ is the status bit that indicates if the unit is in the on or off state. The constant coefficients $a_{0,m}$, $a_{1,m}$, $b_{0,m}$, $c_{0,m}$, $c_{1,m}$, and T_{a} are used to fit the model to the measured winding temperature. The resulting model is a PT1 element where the model parameters depend on the on/off state of the unit. This allows us to consider the different time constants during operation and standstill, which result from, e.g., the machine's cooling system.

2.3. System limits

PSPPs must adhere to several restrictions. As briefly mentioned, most of the technical limits are considered during the development of the efficiency maps. However, additional limits must be considered in the short-term optimization of different electricity markets. The first group is connected to the power limits. Due to cavitation and low efficiency at low powers, the lower power bound in the turbine and pump mode, $P_{\mathrm{t},m}^{\mathrm{lb}}$ and $P_{\mathrm{p},m}^{\mathrm{lb}}$, respectively, are defined by the Francis pump–turbine characteristics [43]. The upper power limits $P_{\mathrm{t},m}^{\mathrm{ub}}$ and $P_{\mathrm{p},m}^{\mathrm{ub}}$ are generally defined as the nominal generator power to prevent electrical overload. However, the maximum power that can be produced depends on the available turbine head [17] and can be lower or larger than the given upper power bound, especially if an electrical overload is allowed. The maximum power in the turbine $P_{\mathrm{t},m}^{\max}(h_{\mathrm{t},m})$ and pump mode $P_{\mathrm{p},m}^{\max}(h_{\mathrm{t},m})$ can be calculated from the detailed plant model together with the efficiency maps. A polynomial approximates these powers to allow for an efficient implementation.

The implementation of the power limits need to consider that Day-Ahead and Intraday optimizations are performed together with optimizing the ancillary services. This means that the PSPP must be able to provide the offered ancillary services, namely the FCR and positive and negative aFRR powers, P_m^{FCR}, $P_m^{\mathrm{aFRR}+}$, $P_m^{\mathrm{aFRR}-}$, respectively, at all times. Thus, the power constraints are given by

$$P_{\mathrm{t},m} - P_m^{\mathrm{FCR}} - P_m^{\mathrm{aFRR}-} \geq P_{\mathrm{t},m}^{\mathrm{lb}} \tag{6a}$$
$$P_{\mathrm{t},m} + P_m^{\mathrm{FCR}} + P_m^{\mathrm{aFRR}+} \leq P_{\mathrm{t},m}^{\mathrm{ub}} \tag{6b}$$
$$P_{\mathrm{t},m} + P_m^{\mathrm{FCR}} + P_m^{\mathrm{aFRR}+} \leq P_{\mathrm{t},m}^{\max}(h_{\mathrm{t},m}) \tag{6c}$$
$$P_{\mathrm{p},m} - P_m^{\mathrm{FCR}} - P_m^{\mathrm{aFRR}+} \geq P_{\mathrm{p},m}^{\mathrm{lb}} \tag{6d}$$
$$P_{\mathrm{p},m} + P_m^{\mathrm{FCR}} + P_m^{\mathrm{aFRR}-} \leq P_{\mathrm{p},m}^{\mathrm{ub}} \tag{6e}$$
$$P_{\mathrm{p},m} + P_m^{\mathrm{FCR}} + P_m^{\mathrm{aFRR}-} \leq P_{\mathrm{p},m}^{\max}(h_{\mathrm{t},m}). \tag{6f}$$

$P_{\mathrm{t},m}$ and $P_{\mathrm{p},m}$ depend on the analyzed market, i.e., they consist of the offered Day-Ahead power in the Day-Ahead market, or the offered Day-Ahead and Intraday powers for the Intraday market. This topic is discussed in detail in the following sections. The plant must also contain reserve energy to provide the desired ancillary services. Thus, additional constraints on the reservoir filling level are necessary. This topic is discussed in more detail in Section 3.1.

The provided ancillary service powers are constrained by upper bounds of the FCR $P^{\mathrm{FCR,ub}}$, and the positive and negative aFRR $P^{\mathrm{aFRR}+,\mathrm{ub}}$ and $P^{\mathrm{aFRR}-,\mathrm{ub}}$ in the form of

$$0 \leq P_m^{\mathrm{FCR}} \leq P_m^{\mathrm{FCR,ub}} \left(s_{\mathrm{t},m}^{\mathrm{da}} + s_{\mathrm{p},m}^{\mathrm{da}}\right) \tag{7a}$$
$$0 \leq P_m^{\mathrm{aFRR}+} \leq P_m^{\mathrm{aFRR}+,\mathrm{ub}} \left(s_{\mathrm{t},m}^{\mathrm{da}} + s_{\mathrm{p},m}^{\mathrm{da}}\right) \tag{7b}$$
$$0 \leq P_m^{\mathrm{aFRR}-} \leq P_m^{\mathrm{aFRR}-,\mathrm{ub}} \left(s_{\mathrm{t},m}^{\mathrm{da}} + s_{\mathrm{p},m}^{\mathrm{da}}\right). \tag{7c}$$

Here, $s_{\mathrm{t}}^{\mathrm{da}}$ and $s_{\mathrm{p}}^{\mathrm{da}}$ are the status bits of the turbine and pump mode, respectively, in the Day-Ahead market. Based on (7), the provision of ancillary services is limited to active units in the Day-Ahead market. This is particularly necessary for the FCR, as the unit must be run cope with grid requirements [16].

Remark 1. PSPP starting times are typically lower than the requested aFRR activation times, making it possible to provide aFRR from a standstill [44]. However, this can result in the requirement that the PSPP provides small values of aFRR, forcing the plant to operate in a hydraulic short circuit. This can be prevented by operating the PSPP on the grid when providing aFRR.

The status bits are binary variables, i.e.,

$$s_{\mathrm{t},m}^{\mathrm{da}}, s_{\mathrm{p},m}^{\mathrm{da}}, s_{\mathrm{t},m}^{\mathrm{id}}, s_{\mathrm{p},m}^{\mathrm{id}} \in \{0,1\} \tag{8}$$

holds. The superscript da indicates the Day-Ahead market, and the superscript id the continuous Intraday market.

The reservoir head h_{g} is limited to prevent spillage or complete discharge

$$h_{\mathrm{g}}^{\mathrm{lb}} \leq h_{\mathrm{g}} \leq h_{\mathrm{g}}^{\mathrm{ub}}, \tag{9}$$

where the lower and upper bounds are referred to with lb and ub, respectively, and are determined by the reservoir construction. Likewise, the upper-temperature limit is given by

$$T_{\mathrm{w},m} \leq T_{\mathrm{w},m}^{\mathrm{ub}}, \tag{10}$$

where the upper-temperature bound $T_{\mathrm{w},m}^{\mathrm{ub}}$ is defined by the generator winding insulation class.

2.4. System model

The overall system model follows from the subsystems in the form of a differential–algebraic system of equations

$$\dot{\boldsymbol{x}} = \boldsymbol{f}(\boldsymbol{x}, \boldsymbol{z}, \boldsymbol{u}) \tag{11a}$$
$$\boldsymbol{0} = \boldsymbol{g}(\boldsymbol{x}, \boldsymbol{z}, \boldsymbol{u}), \tag{11b}$$

with the state $\boldsymbol{x}$, the algebraic variable $\boldsymbol{z}$, and the control input $\boldsymbol{u}$ given by

$$\boldsymbol{x}^T = \left[h_{\mathrm{g}}, T_{\mathrm{w},1}, \ldots, T_{\mathrm{w},4}\right] \tag{12a}$$
$$\boldsymbol{z}^T = \left[q_{\mathrm{t},1}, \ldots, q_{\mathrm{t},4}, q_{\mathrm{p},1}, \ldots, q_{\mathrm{p},4}\right] \tag{12b}$$
$$\boldsymbol{u}^T = \Big[P_{\mathrm{t},1}^{\mathrm{da}}, \ldots, P_{\mathrm{t},4}^{\mathrm{da}}, s_{\mathrm{t},1}^{\mathrm{da}}, \ldots, s_{\mathrm{t},4}^{\mathrm{da}}, P_{\mathrm{p},1}^{\mathrm{da}}, \ldots, P_{\mathrm{p},4}^{\mathrm{da}}, s_{\mathrm{p},1}^{\mathrm{da}}, \ldots, s_{\mathrm{p},4}^{\mathrm{da}}, P_1^{\mathrm{FCR}}, \ldots, P_4^{\mathrm{FCR}}, P_1^{\mathrm{aFRR}+}, \ldots, P_4^{\mathrm{aFRR}+}, P_1^{\mathrm{aFRR}-}, \ldots, P_4^{\mathrm{aFRR}-}, P_{\mathrm{t},1}^{\mathrm{id}}, \ldots, P_{\mathrm{t},4}^{\mathrm{id}}, s_{\mathrm{t},1}^{\mathrm{id}}, \ldots, s_{\mathrm{t},4}^{\mathrm{id}}, P_{\mathrm{p},1}^{\mathrm{id}}, \ldots, P_{\mathrm{p},4}^{\mathrm{id}}, s_{\mathrm{p},1}^{\mathrm{id}}, \ldots, s_{\mathrm{p},4}^{\mathrm{id}} \Big]. \tag{12c}$$

For implementation in the optimization problems, (11) is discretized using the implicit Euler method

$$\boldsymbol{0} = \boldsymbol{x}_{k+1} - \boldsymbol{x}_k - \Delta\tau \boldsymbol{f}\left(\boldsymbol{x}_{k+1}, \boldsymbol{z}_{k+1}, \boldsymbol{u}_k\right) \tag{13a}$$
$$\boldsymbol{0} = \boldsymbol{g}\left(\boldsymbol{x}_{k+1}, \boldsymbol{z}_{k+1}, \boldsymbol{u}_k\right). \tag{13b}$$

Here, k is the discretization step, and $\Delta\tau$ is the constant discretization step size.

3. Day-ahead market with ancillary services

The goal of the optimal dispatch is to maximize the PSPP profit in different markets. As described in Section 1, the Day-Ahead and ancillary services markets are optimized together for optimal plant utilization.

3.1. Optimization task

The Day-Ahead optimization is performed over a week due to the price periodicity and the reservoir size. The optimization interval length is $T = 168$ h, and the step size follows from the hourly offer size as $\Delta\tau = 1$ h, which yields the number of time intervals $K = T/\Delta\tau = 168$. The current plant state gives the initial conditions of the plant

$$\boldsymbol{x}_{k=0} = \boldsymbol{x}_0, \quad \boldsymbol{z}_{k=0} = \boldsymbol{z}_0. \tag{14}$$

Since the profit maximization task would tend to empty the reservoir to generate power, it is enforced that the filling of the reservoir must be kept the same over the week, i.e.,

$$h_{\mathrm{g},0} - h_{\mathrm{g},K} = 0. \tag{15}$$

The powers and status bits used in the power constraints (6) and the model (13) are given as the Day-Ahead powers and status bits

$$P_{\mathrm{t},m,k} = P^{\mathrm{da}}_{\mathrm{t},m,k}, \qquad P_{\mathrm{p},m,k} = P^{\mathrm{da}}_{\mathrm{p},m,k}, \tag{16a}$$

$$s_{\mathrm{t},m,k} = s^{\mathrm{da}}_{\mathrm{t},m,k}, \qquad s_{\mathrm{p},m,k} = s^{\mathrm{da}}_{\mathrm{p},m,k}. \tag{16b}$$

As a result of this choice of the powers and status bits, the states $\boldsymbol{x}$ and algebraic variables $\boldsymbol{z}$ are defined for the Day-Ahead power only, i.e., not taking into account the ancillary service powers. This, however, could violate the gross head and winding temperature constraints, (9) and (10), respectively, if ancillary services are provided. This problem is coped with by calculating the worst-case gross head levels and winding temperatures, assuming a full activation of the ancillary power reserves in the last 4 h, similar to [45]. Here, it is assumed that the effects of the activation are compensated after 4 h by ancillary services activation in the opposite direction or by trading on the continuous Intraday market. The total positive power activation is given as $P^{+}_{m,k} = P_{m,k} + P^{\mathrm{FCR}}_{m,k} + P^{\mathrm{aFRR+}}_{m,k}$ and the negative activation as $P^{-}_{m,k} = P_{m,k} - P^{\mathrm{FCR}}_{m,k} - P^{\mathrm{aFRR-}}_{m,k}$, with $P_{m,k} = P^{\mathrm{da}}_{\mathrm{t},m,k} s^{\mathrm{da}}_{\mathrm{t},m,k} - P^{\mathrm{da}}_{\mathrm{p},m,k} s^{\mathrm{da}}_{\mathrm{p},m,k}$. The maximum and minimum gross head $h^{+}_{\mathrm{g},k}$ and $h^{-}_{\mathrm{g},k}$ are calculated with the powers $P^{+}_{m,k}$ and $P^{-}_{m,k}$ and the efficiency of the Day-Ahead powers and pump–turbine heads, $\eta_{\mathrm{t},m}(P^{\mathrm{da}}_{\mathrm{t},m,k}, h^{\mathrm{da}}_{\mathrm{t},m,k})$ and $\eta_{\mathrm{p},m}(P^{\mathrm{da}}_{\mathrm{p},m,k}, h^{\mathrm{da}}_{\mathrm{t},m,k})$, respectively, to reduce computation time, see (1)–(4). The maximum winding temperature $T^{+}_{\mathrm{w},m,k}$ is calculated assuming the maximum apparent power, see (5). This results in additional gross head and winding temperature constraints in the form of

$$h^{\mathrm{lb}}_{\mathrm{g}} \le h^{+}_{\mathrm{g},k} \le h^{\mathrm{ub}}_{\mathrm{g}} \tag{17a}$$

$$h^{\mathrm{lb}}_{\mathrm{g}} \le h^{-}_{\mathrm{g},k} \le h^{\mathrm{ub}}_{\mathrm{g}} \tag{17b}$$

$$T^{+}_{\mathrm{w},m,k} \le T^{\mathrm{ub}}_{\mathrm{w},m}. \tag{17c}$$

The Day-Ahead optimization task with ancillary services is formulated as follows

$$\begin{aligned} \max_{\boldsymbol{X}} \sum_{k=0}^{K-1} \sum_{m=1}^{M} \Big(& \left(c^{\mathrm{da}}_{k} - c^{\mathrm{t}}\right) P^{\mathrm{da}}_{\mathrm{t},m,k} s^{\mathrm{da}}_{\mathrm{t},m,k} - \left(c^{\mathrm{da}}_{k} + c^{\mathrm{p}}\right) P^{\mathrm{da}}_{\mathrm{p},m,k} s^{\mathrm{da}}_{\mathrm{p},m,k} \\ & + c^{\mathrm{FCR}}_{k} P^{\mathrm{FCR}}_{m,k} + c^{\mathrm{aFRR+}}_{k} P^{\mathrm{aFRR+}}_{m,k} + c^{\mathrm{aFRR-}}_{k} P^{\mathrm{aFRR-}}_{m,k} \\ & - p^{\mathrm{da}}_{\mathrm{ss},m,k} \Big) \Delta\tau, \end{aligned} \tag{18}$$

subject to (6)–(10), and (13)–(17). All optimization variables are summarized in $\boldsymbol{X}$

$$\boldsymbol{X}^T = \left[\boldsymbol{X}^T_0, \ldots, \boldsymbol{X}^T_K\right], \tag{19}$$

with $\boldsymbol{X}^T_k = \left[\boldsymbol{x}^T_k, \boldsymbol{z}^T_k, \boldsymbol{u}^T_k\right]$. Here, c^{da}_k is the (predicted) Day-Ahead market price, and c^{FCR}_k, $c^{\mathrm{aFRR+}}_k$, and $c^{\mathrm{aFRR-}}_k$ are the prices for FCR and positive and negative aFRR, respectively. Moreover, c^{t} and c^{p} are the withdrawal and feed-in tariffs. The term $p^{\mathrm{da}}_{\mathrm{ss},m,k}$ denotes the additional costs resulting from wear and tear during the start and stop of the unit [46], defined as

$$\begin{aligned} p^{\mathrm{da}}_{\mathrm{ss},m,k} = c_{\mathrm{ss}} \big(& s^{\mathrm{da}}_{\mathrm{t},m,k} - 2 s^{\mathrm{da}}_{\mathrm{t},m,k} s^{\mathrm{da}}_{\mathrm{t},m,k+1} + s^{\mathrm{da}}_{\mathrm{t},m,k+1} \\ & + s^{\mathrm{da}}_{\mathrm{p},m,k} - 2 s^{\mathrm{da}}_{\mathrm{p},m,k} s^{\mathrm{da}}_{\mathrm{p},m,k+1} + s^{\mathrm{da}}_{\mathrm{p},m,k+1} \big), \end{aligned} \tag{20}$$

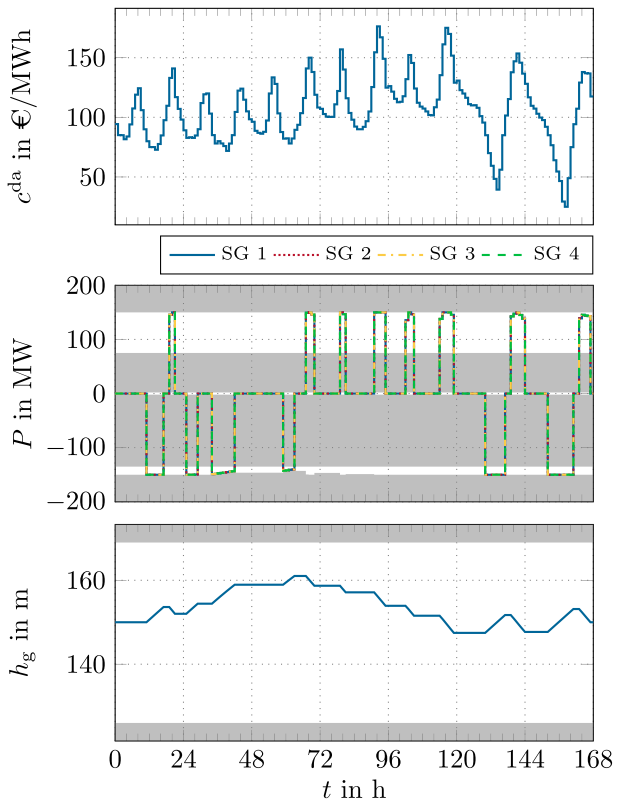

Fig. 3. Optimal operation of four synchronous generators in the Day-Ahead market for week 24 of 2023 in Austria. The infeasible area is shaded gray.

with the cost of every start and stop c_{ss}.

No assumptions about the Intraday market are made in (18), i.e., $P^{\mathrm{id}}_{\mathrm{t},m,k} = P^{\mathrm{id}}_{\mathrm{p},m,k} = s^{\mathrm{id}}_{\mathrm{t},m,k} = s^{\mathrm{id}}_{\mathrm{p},m,k} = 0$ applies.

The model and optimization tasks were implemented in MATLAB R2019A with CASADI 3.6.1 [47]. The optimization problem was solved on an AMD Ryzen 7 3800X 8-Core CPU with 32-GB RAM using the hybrid Quesada-Grossman method [48] in Artelys Knitro [49].

3.2. Results

The optimal operation of a plant with four synchronous generators is studied in the first step. The results of the Day-Ahead market without ancillary services of the calendar week 24 of 2023 for Austria are given in Fig. 3. The results show that all generators are operated with exactly the same power during the whole week near the maximum (nominal) power P in the turbine mode. This is due to the high energy prices in these intervals and the high efficiency of the SG at nominal power. The generators are operated at lower powers only in times of lower energy prices, during which it is still economical to sell energy. In pumping mode, the generators are always operated at maximum power due to the significantly lower efficiency at lower powers of fixed-speed Francis pump–turbines, see [17]. The maximal producible power in the pump mode $P^{\mathrm{max}}_{\mathrm{p}}(h_{\mathrm{t}})$ also changes due to pump–turbine head h_{t} changes, see Fig. 3. It can also be seen that the plant is out of operation for a long time. The plant adheres to the operating limits of the reservoir, and the goal of the same head at the beginning and the end of the optimization interval is also reached, see Fig. 3. The PSPP achieves a profit of 0.732 M€ in the considered week.

As briefly discussed in the previous sections, operating the plant with a power larger than the nominal power is possible and might be beneficial. This is also visible in Fig. 3, as the plant operates with the maximum allowable power if the prices are high (turbine mode) or

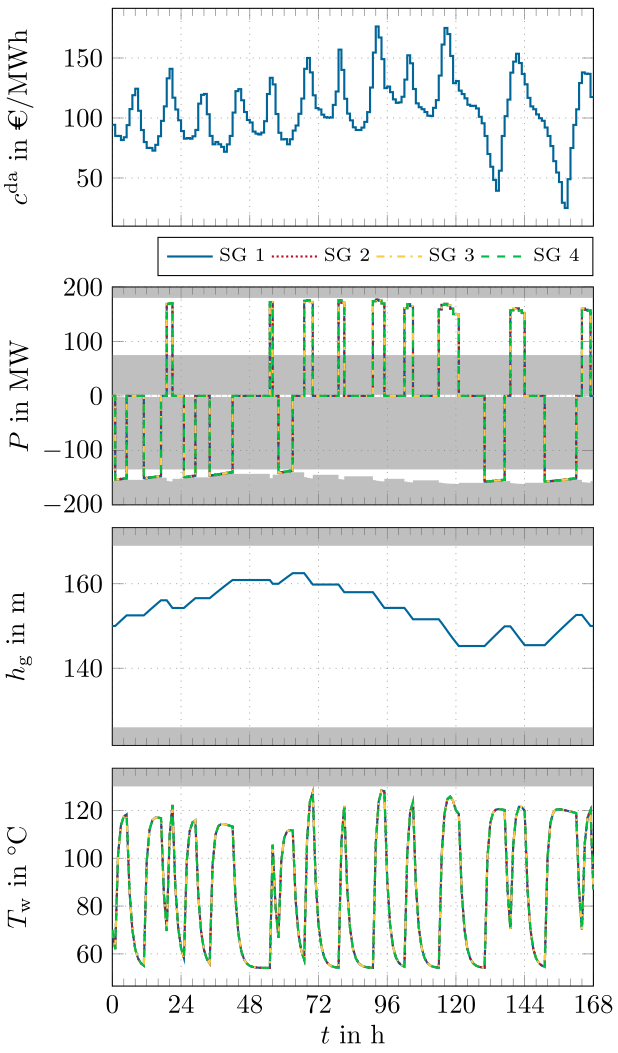

Fig. 4. Optimal operation of four synchronous generators in the Day-Ahead market with an allowed electrical overload of 20 % for week 24 of 2023 in Austria. The infeasible area is shaded gray.

low (pump mode). Thus, the results of an allowed overload of 20 %, at which the generators cannot be operated continuously due to the winding temperature limits, are depicted in Fig. 4. The plant operates with higher powers in this case. It is visible that the generators' thermal limit is only reached for a very short time, and a safe distance is present for the most part. The changes in the gross head are also more significant compared to Fig. 3 due to the higher amount of processed energy. The total profit with an allowed overload of 20 % is 0.827 M€ for the same plant and week, constituting a profit increase of 13.03 % compared to the case without an electrical overload. Note that the profit increase depends on the considered week. The authors have observed profit increases of up to 20 % for weeks with significant price differences, but the mean profit increase over multiple years has a value of 16.76 %. These results clearly show the possible benefits of an electrical overload. Therefore, all the following results are given for the case with an electrical overload.

The previous results only assume operation in the Day-Ahead market. Fig. 5 depicts the optimal operation in the Day-Ahead, FCR, and aFRR markets of the same plant equipped with four doubly-fed induction machines to show the additional flexibility of variable-speed units in the pumping mode. The Day-Ahead powers are given as lines, whereas the colored shaded areas of the time evolutions refer to reserves maintained for the ancillary services. In times of high Day-Ahead and low ancillary service prices, the plant operates with high power to utilize price arbitrage. However, if the ancillary services price is high, the plant operates with a reduced Day-Ahead power to provide more ancillary services, particularly aFRR. The provision of ancillary services requires large reserves in the temperature (colored shaded areas), but the gross head reserves are negligible and hardly visible due to the reservoir size. The units additionally operate in the hydraulic short-circuit mode. The reasons are the high aFRR and noncompetitive Day-Ahead prices. Therefore, it is not economical to operate the units in the turbine or pump mode, resulting in a short-circuit operation to provide ancillary services. The DFIMs are also not operated synchronously here. For instance, not all units are active at $t = 49$ h due to the high reservoir filling level and the less competitive Day-Ahead price. The extended operating range of the DFIM and the additional income from the ancillary service markets result in a revenue of 2.012 M€ for the considered week. The profits for different generator combinations in the Day-Ahead and ancillary service markets are compared in Fig. 6. The results show that variable-speed technology achieves higher profits than fixed-speed SGs. This is particularly true for the plant with four DFIMs, which has higher profits than CFSGs due to lower converter losses at high powers [17]. The provision of ancillary services additionally increases the profit, especially in the case of variable-speed generators and the provision of aFRR. The reason is the extended operating range and the possibility of providing ancillary services in the pump mode. Note also that only a small benefit exists in providing only FCR and almost no benefit in providing FCR in addition to aFRR. This comes from the higher aFRR prices and the limited reserves. The profit of a plant where two variable- and two fixed-speed units are combined lies between the plant's profit with SGs and the respective variable-speed technology. It must be noted that the given Day-Ahead optimization with ancillary services (18) only considers the power price for the aFRR. However, an energy price also exists, which creates additional profits if the service is activated. This aspect is not taken into account in this work. Fig. 6 also shows the optimization times. They are between 15 s (no ancillary services) and 60 s (with ancillary services). These computation times are significantly shorter than in [2], where similar hardware was used but a less detailed model. This allows for utilizing the optimization task for real-time trading in the electricity market by developing a bidding strategy based on the Day-Ahead optimization, see Section 5.

4. Intraday market

The goal of trading in the Intraday market is to utilize unused power reserves from the Day-Ahead market or the ancillary service markets to generate additional profits utilizing the high price volatility of the Intraday market [13]. In this work, trading is performed only on the continuous Intraday market, and the traded powers from the previous markets are considered in the optimization.

4.1. Optimization task

Quarter-hourly products are traded continuously throughout the day in the continuous Intraday market in quarter-hourly intervals. The Intraday optimization is, therefore, a moving horizon optimization within the day with a sampling time and a time discretization of $\Delta\tau = 1/4$ h. The system is thus evaluated at $t = n\Delta\tau$, $n \in \mathbb{N}_0$, with the prediction horizon $[n\Delta\tau, n\Delta\tau + T]$. The time horizon $T = K\Delta\tau$ is chosen as $T = 4$ h ($K = 16$), which proved meaningful as it is long enough to exploit the price volatility while allowing for short computation times. The initial states for the optimization at time step n are given as

$$\boldsymbol{x}_{n|0} = \boldsymbol{x}_n, \quad \boldsymbol{z}_{n|0} = \boldsymbol{z}_n, \tag{21}$$

where the index $n|k$ denotes the discretization step k of the prediction horizon evaluated at the trading time step n.

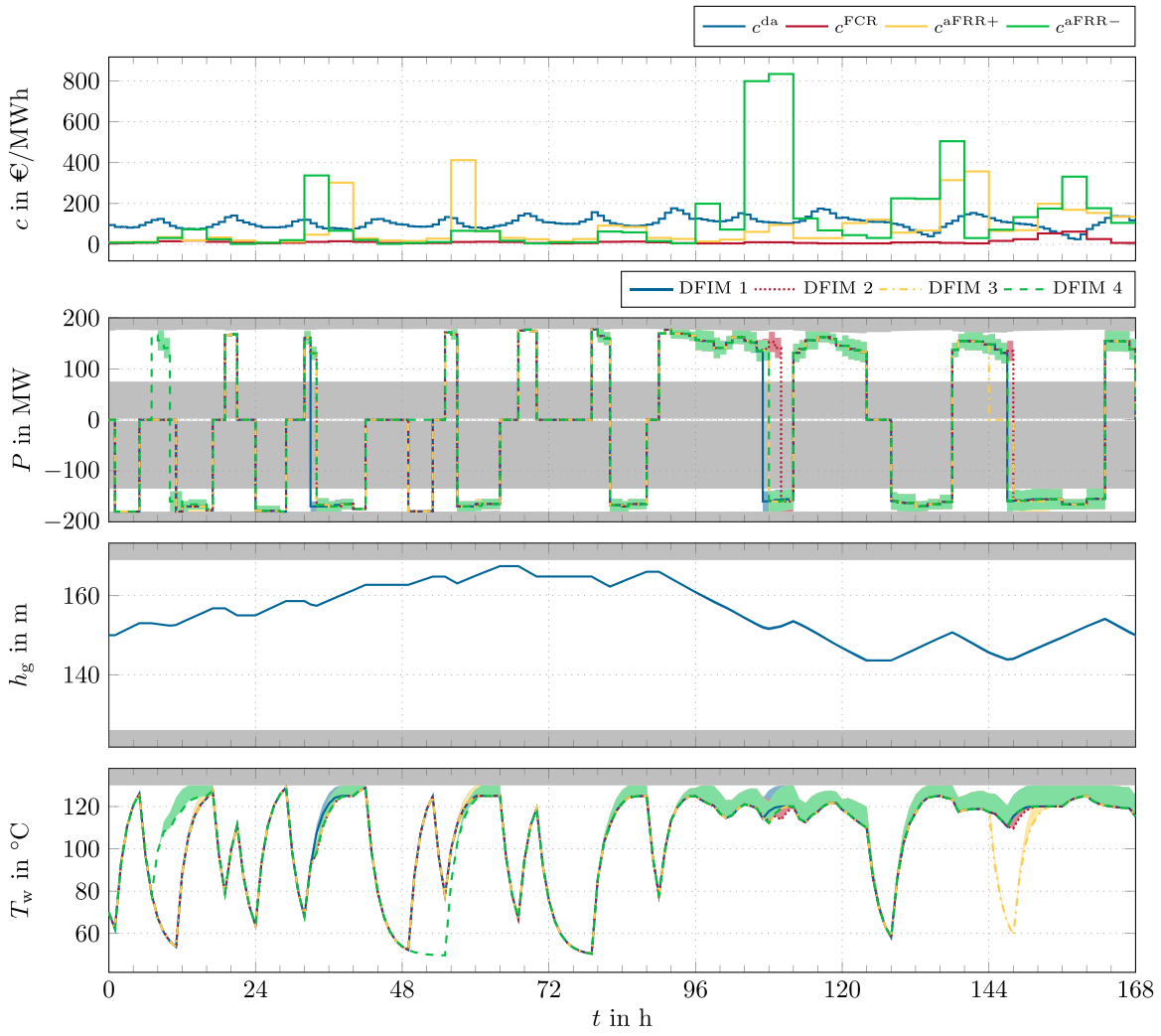

Fig. 5. Optimal operation of four doubly-fed induction machines in the Day-Ahead market with FCR and aFRR for week 24 of 2023 in Austria. The infeasible area is shaded gray.

The powers and status bits of the power constraints (6) and the model (13) are given by the Day-Ahead and Intraday powers and status bits

$$P_{\mathrm{t},m,n|k} = P^{\mathrm{da}}_{\mathrm{t},m,n|k} s^{\mathrm{da}}_{\mathrm{t},m,n|k} + \sum_{j=0}^{K-k} P^{\mathrm{id}}_{\mathrm{t},m,n-j|k+j} \tag{22a}$$

$$P_{\mathrm{p},m,n|k} = P^{\mathrm{da}}_{\mathrm{p},m,n|k} s^{\mathrm{da}}_{\mathrm{p},m,n|k} + \sum_{j=0}^{K-k} P^{\mathrm{id}}_{\mathrm{p},m,n-j|k+j} \tag{22b}$$

$$s_{\mathrm{t},m,n|k} = s^{\mathrm{da}}_{\mathrm{t},m,n|k} \vee s^{\mathrm{id}}_{\mathrm{t},m,n|k} \vee \ldots \vee s^{\mathrm{id}}_{\mathrm{t},m,n-K|k+K} \tag{22c}$$

$$s_{\mathrm{p},m,n|k} = s^{\mathrm{da}}_{\mathrm{p},m,n|k} \vee s^{\mathrm{id}}_{\mathrm{p},m,n|k} \vee \ldots \vee s^{\mathrm{id}}_{\mathrm{p},m,n-K|k+K}, \tag{22d}$$

where traded powers from the current and previous trading iterations are considered. The Intraday optimization is given by

$$\begin{aligned} \max_{\boldsymbol{X}} \sum_{k=0}^{K-1} \sum_{m=1}^{M} \Big(& \left(c^{\mathrm{id}}_{n|k} - c^{\mathrm{t}}\right) P^{\mathrm{id}}_{\mathrm{t},m,n|k} s^{\mathrm{id}}_{\mathrm{t},m,n|k} \\ & - \left(c^{\mathrm{id}}_{n|k} + c^{\mathrm{p}}\right) P^{\mathrm{id}}_{\mathrm{p},m,n|k} s^{\mathrm{id}}_{\mathrm{p},m,n|k} - p^{\mathrm{id}}_{\mathrm{ss},m,n|k} \\ & + w_1 \left(\max\left(T_{\mathrm{w},m,n|k} - T^{\mathrm{ub}}_{\mathrm{w},m}, 0\right)\right)^2 \\ & + w_1 \left(\max\left(T^{+}_{\mathrm{w},m,n|k} - T^{\mathrm{ub}}_{\mathrm{w},m}, 0\right)\right)^2 \Big) \, \Delta\tau \\ & + w_2 \left(h_{\mathrm{g},n|K} - h^{\mathrm{da}}_{\mathrm{g},n|K}\right)^2, \end{aligned} \tag{23}$$

subject to (6)–(9), (13), (17a), (17b), (21), and (22). Here, $c^{\mathrm{id}}_{n|k}$ is the Intraday price, c^{t} and c^{p} are the withdrawal and feed-in tariffs, and $p^{\mathrm{id}}_{\mathrm{ss},m,n|k}$ are the start and stop costs defined equivalently to (20). The first two terms in the cost function represent the Intraday market profit, and the third term are the start and stop costs. The fourth and fifth terms are penalty functions for the maximum allowable winding temperature. The last term aims to keep the reservoir filling level close to the results of the Day-Ahead market $h^{\mathrm{da}}_{\mathrm{g},n|K}$. This is necessary to prevent the reservoir from discharging and to be able to provide the sold Day-Ahead and ancillary service powers. Note that this term also allows to compensate for a reservoir filling level mismatch due to the activation of ancillary services.

Remark 2. The last three cost function terms could be implemented as hard constraints. However, model inaccuracies may result in discrepancies between the projected and obtained plant trajectories. The optimization problem (23) could then be infeasible as it might be impossible to compensate for these errors. For example, if the SG is operating in pump mode with maximum power, but the requested end filling level requires additional pumping power, reaching the requested filling level would be impossible. The given optimization problem compensates for this by operating the plant as close as possible to the desired filling level, which is accomplished by a suitable choice of the weighting factors w_1, $w_2 > 0$.

The Intraday optimization's ancillary services limits (17) are calculated with the power $P_{m,n|k} = P^{\mathrm{da}}_{\mathrm{t},m,n|k} s^{\mathrm{da}}_{\mathrm{t},m,n|k} + \sum_{j=0}^{K-k} P^{\mathrm{id}}_{\mathrm{t},m,n-j|k+j} s^{\mathrm{id}}_{\mathrm{t},m,n-j|k+j} -$

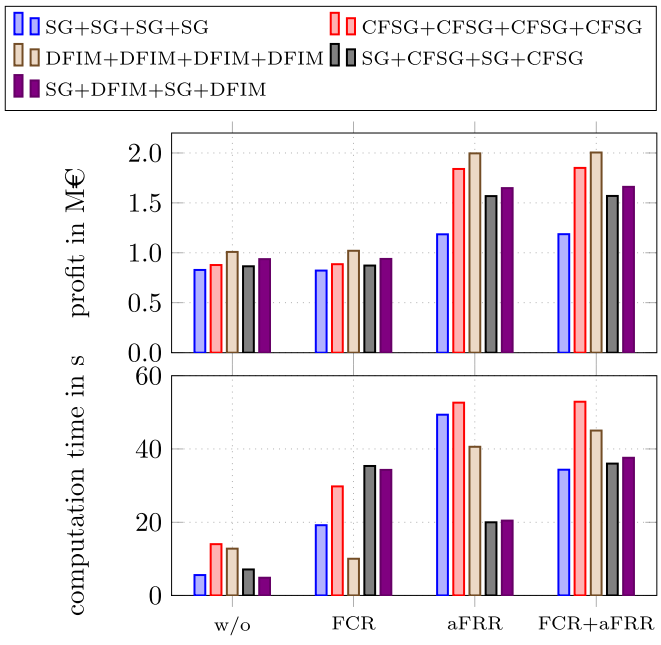

Fig. 6. Profits and computation times for different generator combinations in the Day-Ahead and ancillary service markets for week 24 of 2023 in Austria.

$P^{\mathrm{da}}_{\mathrm{p},m,n|k} s^{\mathrm{da}}_{\mathrm{p},m,n|k} - \sum_{j=0}^{K-k} P^{\mathrm{id}}_{\mathrm{p},m,n-j|k+j} s^{\mathrm{id}}_{\mathrm{p},m,n-j|k+j}$. Note that the Day-Ahead and ancillary services powers and status bits are obtained by solving (18), and they are known for Intraday trading. They are, therefore, fixed in this optimization stage.

4.2. Results

The optimal operation in the Intraday market without ancillary services is studied for only one active CFSG to show the additional flexibility of variable-speed units in the pump mode. Fig. 7 shows the results, where the previously traded Day-Ahead and the Intraday powers traded at the trading times $t = 0$ and $t = 0.25$ h are given. The weighted average price of the Austrian Intraday market for week 24 of 2023 was used here. The price shows the high volatility of the market. The plant is started in the turbine mode to sell additional power during the high price interval and in the pump mode to buy power during intervals of low price. The plant also sells additional power during the pumping mode operation by reducing the pumping power from the Day-Ahead market to utilize high price intervals. It is also important to note that the plant adheres to all operational limits. Tracking the Day-Ahead reservoir level is crucial to utilize the reservoir optimally. It is important to note that the plant utilizes most of its flexibility for trading at $t = 0$, while only minor trading is performed at the moment $t = 0.25$ h. This comes from the fact that the plant is operated to follow the Day-Ahead schedules and that the unit's flexibility is limited in the pump mode operation, even with variable-speed operation. The total profit is 994 € for the powers traded at the trading time $t = 0$ and 6 € at $t = 0.25$ h. In Fig. 8, the influence of different generators (SG, DFIM, CFSG) on the additional revenue of the Intraday market is studied. The significantly smaller flexibility of the fixed-speed SG in the pump mode results in smaller revenues from the Intraday market. Additionally, the income from the Intraday market is reduced if ancillary services are offered with the Day-Ahead market. Interestingly, the total income for all generator combinations from the Day-Ahead, ancillary services, and Intraday market is lower if FCR is offered than in cases without FCR. Moreover, the profit is in most cases lower if FCR and aFRR are offered compared to the case where only aFRR is offered. This comes from the reduced flexibility in the Intraday market due to the necessary power

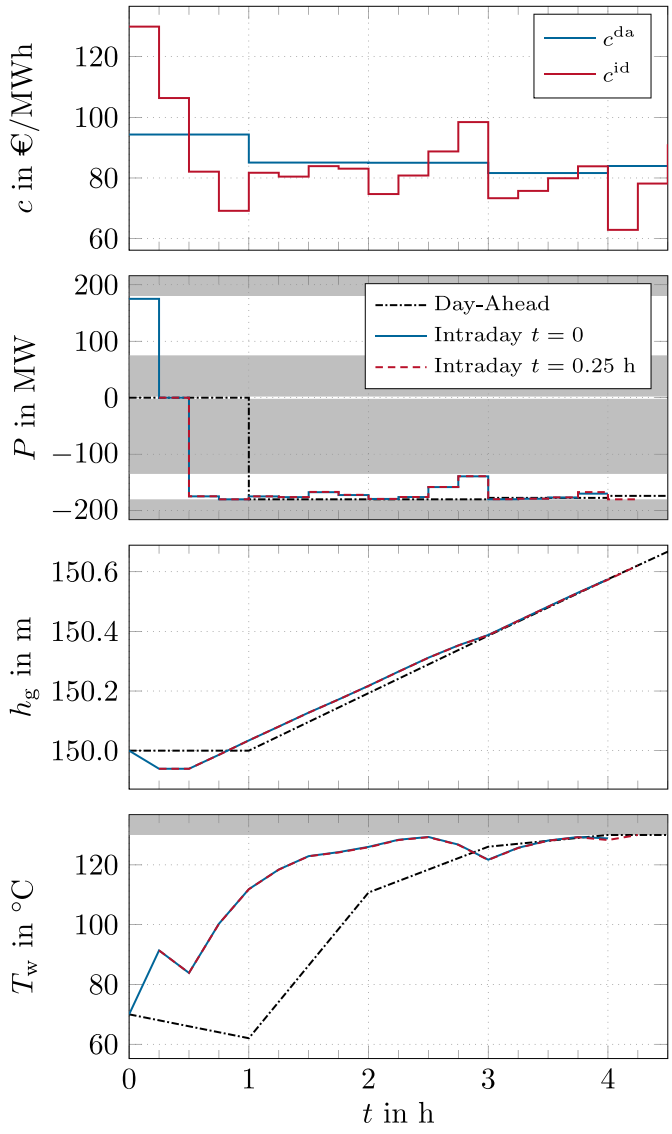

Fig. 7. Optimal Intraday operation of the considered plant with only one active CFSG. The infeasible area is shaded gray.

reserves for the ancillary services, see (6). It, however, must be noted that this strongly depends on the current prices in the different markets. Therefore, the authors have observed weeks in the Austrian energy market where increased total profits are obtained if FCR is offered. However, the results show that it is optimal to offer aFRR, and that a plant equipped with DFIMs is the optimal choice regarding total profit. A thorough study of the investment, operational, and maintenance costs is needed to choose the best generator combination for the plant.

5. Bidding curve generation

The previous sections showed the optimal plant operation in the electricity market for a given price. As briefly discussed in Section 1, the price is not known in advance. This section thus presents a bidding curve generation strategy for PSPPs based on the optimization task presented in Section 3. The bidding curve generation performs a robust optimization as presented, e.g., in [35]. To do so, a prediction of the price confidence interval in the Day-Ahead market is required, which can be obtained from price prediction methods as, e.g., given in [36], see the transparent blue area in Fig. 9. The confidence interval is divided into multiple sub-intervals, where turbine and pump mode

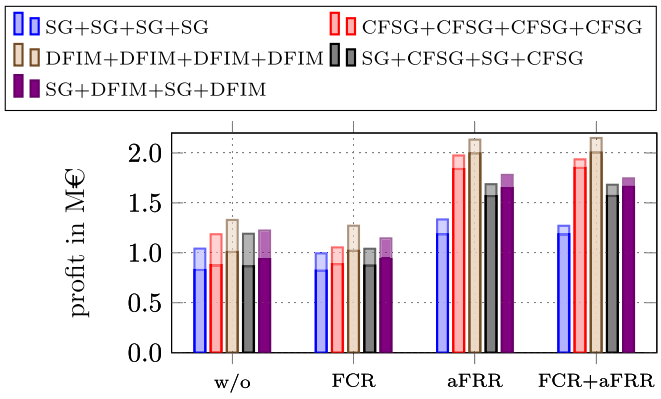

Fig. 8. Profits for different generator combinations in the Day-Ahead, ancillary service, and Intraday markets for week 24 of 2023 in Austria. The additional profit from the Intraday market is marked by transparent colors.

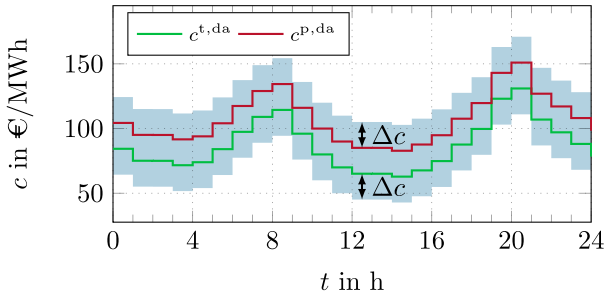

Fig. 9. Predicted price interval (transparent blue) with the used prices for the turbine and pump mode operation $c^{\mathrm{t,da}}$ and $c^{\mathrm{p,da}}$, respectively. The price offset Δc is constant over the horizon.

price profiles are fixed for each sub-interval. Here, the turbine mode price $c^{\mathrm{t,da}}$ is determined by an offset Δc above the minimum price, and the pump mode price $c^{\mathrm{p,da}}$ by an offset Δc below the maximum price, see Fig. 9. The different sub-intervals are given for different values of $\Delta c \in [0, \Delta c_{\max}]$, where $\Delta c_{\max}$ is the width of the price confidence interval. The sub-interval with $\Delta c = 0$ presents the most pessimistic prediction, i.e., a high price during consumption and a low price during generation, whereas $\Delta c = \Delta c_{\max}$ presents the most optimistic prediction. This procedure results in a fixed price for each given value of Δc enabling a deterministic optimization to generate a single point in the bidding curves. The following sections describe the needed steps to generate whole curves. For the sake of simplicity, only the curve generation in the Day-Ahead market is described. The ancillary service markets in Austria are cleared before the Day-Ahead market. Thus, the results of ancillary service markets are known before the Day-Ahead trading, and they can be taken into account by requiring the plant to run when ancillary services are provided and holding the sold reserves free.

5.1. Optimization task

The previously described procedure reduces the generation of bidding curves to a set of deterministic optimizations. These optimizations are based on the optimization problem (18), with minor differences to ensure feasible plant behavior. The first difference is related to the feasible power range. Differences in the predicted and the realized price will yield deviations of h_{t} from the predicted pump–turbine head, influencing the maximum producible power. This uncertainty is taken into account by changing (6c) and (6f) to

$$P_{\mathrm{t},m,k} \leq P^{\max}_{\mathrm{t},m}(h_{\mathrm{t},m,k}) - \Delta P^{\mathrm{b}}_{\mathrm{t},m} \tag{24a}$$

$$P_{\mathrm{p},m,k} \leq P^{\max}_{\mathrm{p},m}(h_{\mathrm{t},m,k}) - \Delta P^{\mathrm{b}}_{\mathrm{p},m}, \tag{24b}$$

where $\Delta P^{\mathrm{b}}_{\mathrm{t},m} > 0$ and $\Delta P^{\mathrm{b}}_{\mathrm{p},m} > 0$ are power reserves in the turbine and pump mode, respectively. The inequalities (6a), (6b), (6d), and (6e) remain unchanged. The uncertainty in the gross head h_{g} is taken into account by changing (9) to

$$h^{\mathrm{lb}}_{\mathrm{g}} + \gamma_k \Delta h^{\mathrm{b}}_{\mathrm{g}} \leq h_{\mathrm{g},k} \leq h^{\mathrm{ub}}_{\mathrm{g}} - \gamma_k \Delta h^{\mathrm{b}}_{\mathrm{g}}, \tag{25}$$

with the gross head reserve $\Delta h^{\mathrm{b}}_{\mathrm{g}} > 0$ and the time-dependent weight γ_k defined as

$$\gamma_k = \begin{cases} \frac{k}{24} & \text{for } 0 \leq k < 24 \\ 1 & \text{for } 24 \leq k < 144 \\ \frac{168-k}{24} & \text{for } 144 \leq k \leq 168. \end{cases} \tag{26}$$

The gross head reserve $\Delta h^{\mathrm{b}}_{\mathrm{g}}$ aims to include a safety margin in the gross head h_{t}. However, this safety margin can be violated during operation, leading to a new and infeasible initial condition in the case of a constant safety margin over the whole prediction interval, see (14). This is prevented by linearly increasing the weight γ_k during the first day. The weight is also linearly reduced during the last day to adhere to the reservoir end filling level constraint (15). Finally, the temperature constraint (10) is changed to

$$T_{\mathrm{w},m,k} \leq T^{\mathrm{ub}}_{\mathrm{w},m} - \gamma_k \Delta T^{\mathrm{b}}_{\mathrm{w},m}, \tag{27}$$

with the temperature reserve $\Delta T^{\mathrm{b}}_{\mathrm{w},m} > 0$. The resulting optimization problem is given by

$$\max_{\boldsymbol{X}_l} \sum_{k=0}^{K-1} \sum_{m=1}^{M} \Big(\Big(c^{\mathrm{t,da}}_{k,l} - c^{\mathrm{t}} \Big) P^{\mathrm{da}}_{\mathrm{t},m,k,l} s^{\mathrm{da}}_{\mathrm{t},m,k,l} - \Big(c^{\mathrm{p,da}}_{k,l} + c^{\mathrm{p}} \Big) P^{\mathrm{da}}_{\mathrm{p},m,k,l} s^{\mathrm{da}}_{\mathrm{p},m,k,l} - p^{\mathrm{da}}_{\mathrm{ss},m,k,l} \Big) \Delta\tau, \tag{28}$$

subject to (8), (13)–(16), (24), (25), and (27).

The optimization problem (28) is solved for a sequence of different values of Δc_l and, therefore, for different price profiles $c^{\mathrm{t,da}}_l$ and $c^{\mathrm{p,da}}_l$, $l = 0, \ldots, L$, where L is the number of price–power pairs in the bidding curves. The given optimization problems are decoupled. In contrast, additional constraints are introduced to guarantee non decreasing bidding curves in [35]. This, however, couples the optimization task l with the results from $l-1$, which requires a solution of the optimization tasks in series, whereas the proposed concept allows the solving of the optimization tasks in parallel. The result is a faster generation of the bidding curves compared to [35], cf. the computation times in Fig. 6. A drawback of this approach is that the resulting bidding curves must be post-processed to ensure non decreasing bidding curves. The post-processing is based on an affine function's least-squares (LS) fit, with the constraint that the offered power is non decreasing, i.e., $\mathrm{d}c^{\mathrm{da}}/\mathrm{d}P_{\mathrm{pspp}} \geq 0$. Note that an LS fit is performed independently for every number of active units due to the high power differences if an additional unit is started. The results of the initial and the post-processed bidding curves are given in Fig. 10, where one LS fit is performed for two active units (LS 1) and a second fit for four active units (LS 2) of the demand curve of a plant consisting of two SGs and two DFIMs for week 24 of 2023 in Austria. A similar procedure is performed in the supply curve for two (LS 3), three (LS 4), or four (LS 5) active units.

These post-processed curves are delivered to the market. The plant receives a plant schedule based on the traded powers of each hour due to the clearing and settlement. A post-optimization is performed to ensure optimal plant operation for the day with the obtained schedule. The goal of the post-optimization is to supply the required plant powers with minimum losses, i.e., with the maximum gross head at the end of the optimization interval. This is formulated as

$$\max_{\boldsymbol{X}} \quad h_{\mathrm{g},K} - w_3 \sum_{k=0}^{23} \sum_{m=1}^{M} p^{\mathrm{da}}_{\mathrm{ss},m,k} \Delta\tau, \tag{29a}$$

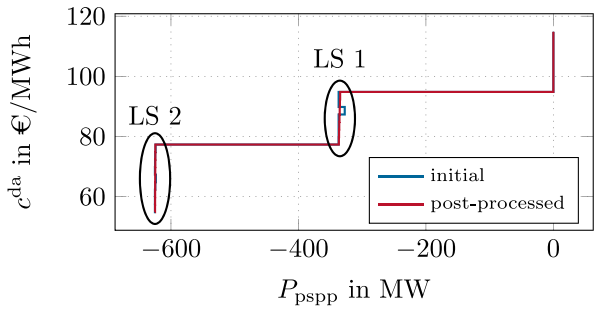

(a) Aggregated demand curve of the plant for $t = 17$ h.

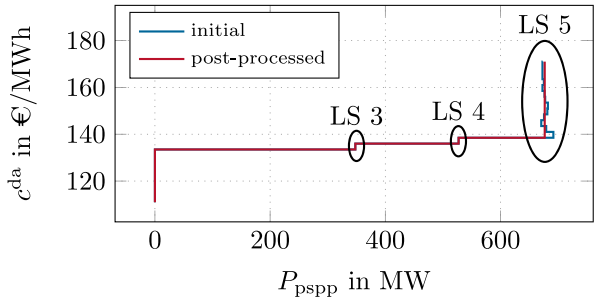

(b) Aggregated supply curve of the plant for $t = 21$ h.

Fig. 10. Initial and post-processed demand and supply curve of a plant consisting of two SGs and two DFIMs for week 24 of 2023 in Austria.

subject to

$$P_{\mathrm{pspp},k} = P_{\mathrm{c\&s},k}, \quad k = 0, \dots, 23, \tag{29b}$$

and (6), (8)–(10), (13), (14), and (16). Here, $P_{\mathrm{c\&s},k}$ is the resulting power from the clearing and settlement for the hour k, i.e., the plant schedule for the following day. The second term in the cost function, which is weighted with a small weighting factor $w_3 > 0$, prevents units from unnecessary state switching, i.e., providing the plant power with the same generators in adjacent intervals is desired to reduce start and stop costs. The time discretization in (29) is chosen as $\Delta\tau = 1$ h and the time horizon as 24 h, i.e., the plant schedule is optimized for the next day.

Remark 3. The post-optimization can be performed multiple times during the day to compensate for model-plant mismatches and activations of ancillary services if offered. Only one post-optimization is performed here, as the previously named effects are not considered.

The overall bidding curve generation strategy is depicted in Fig. 11.

5.2. Results

The results of the bidding curve generation strategy for a plant consisting of two SGs and two DFIMs for week 24 of 2023 in Austria are given in Fig. 12, where the bidding curve generation was performed every day independently. The realized price is equal to the market clearing and settlement price, and the price prediction is obtained by adding a zero-mean normally distributed random value to every 4 h block with a standard deviation of $\sigma = 10$ €/MWh to the realized price, and subsequently filtering the data to obtain smoothly perturbed data. The confidence interval width is $\Delta c_{\max} = 60$ €/MWh, and the price offsets are obtained as $\Delta c_l = l\Delta c_{\max}/L$ with $L = 24$. The results show that the plant is utilized for pumping in intervals with low prices, while the plant is in generating mode for high prices. Note that the plant is operated in short-circuit mode at $t = 153$ h. The reason is the price prediction error which results in a difference between the predicted and realized gross head h_{g}. Two units cannot provide the offered pumping power, forcing three units to operate in the pump mode and one in the turbine mode. The short-circuit operation could be prevented by increasing the power safety margins, which would result in lower revenues. The short-circuit operation could also be prevented by trading on the Intraday market (continuous or auction), resulting only in the operation of two units and with a minimum loss of revenue. The results in Fig. 12 also prove that all physical plant limits are well respected.

Table 1
Profits of different generator combinations in the Austrian Day-Ahead Market in 2019 under the proposed bidding curve generation strategy.

Generators	Profit in M€
SG+SG+SG+SG	8.023
CFSG+CFSG+CFSG+CFSG	9.669
DFIM+DFIM+DFIM+DFIM	11.134
SG+CFSG+SG+CFSG	9.227
SG+DFIM+SG+DFIM	10.515

The proposed bidding curve generation strategy generates a profit of 1.557 M€ in week 24 of 2023 in Austria, while the maximum possible profit with the realized price is 1.619 M€ if optimizing the whole week with exact a priori knowledge of the realized price. Therefore, the proposed bidding generation strategy allows for high profits even under price uncertainty.

It must be noted that the gross head $h_{\mathrm{g},K}$ at the end of the week is not equal to the initial condition and thus violates the constraint (15). This results from the fact that the plant schedule depends on the clearing and settlement process and, thus, also on the competitors that cannot be accurately represented in the optimization task. A simulation over eight weeks was performed to study this effect in more detail, where it is assumed that the same price variation over time is present for all weeks. The results in Fig. 13 show that the gross head h_g converges to a quasi-stationary curve after a few weeks, proving that unreasonable reservoir emptying is prevented. This quasi-stationary curve is close to the optimal curve that would be obtained if the gross head at the beginning (or end) of the week were added to the optimization (depicted in green in Fig. 13). Thus, the trend to reduce the gross head from week 1 to week 8 is consistent with the optimal management of the reservoir level and yields an additional profit of approximately 14 k€ (1.23%) compared to the initial head level. The main reason for this effect is the influence of the gross head on the units' efficiency.

The performance of different generator types under the proposed bidding curve generation strategy in the Day-Ahead market is given in Table 1. The results are presented for 2019 in the Austrian market due to significant price changes from 2020 to 2023. The results follow the Day-Ahead results from Section 3. A significant difference is that the yearly profits in 2019 are low compared to the weekly profits from Section 3, due to the mentioned market changes.

6. Conclusions

This paper studied the optimal operation of pumped storage power plants (PSPP) in different electricity markets. A detailed PSPP model was developed, which takes all essential effects into account: (i) the gross head and power influence on the units' efficiency, (ii) the head influence on the maximal producible power, (iii) the reservoir limits, (iv) the generators' thermal limits, (v) the head losses in the pipeline, and (vi) the start and stop costs. The result is a nonlinear plant model that can be implemented efficiently and flexibly to adapt to different plant topologies, including different generator types and even heterogeneous plants, i.e., plants consisting of variable- and fixed-speed generator types.

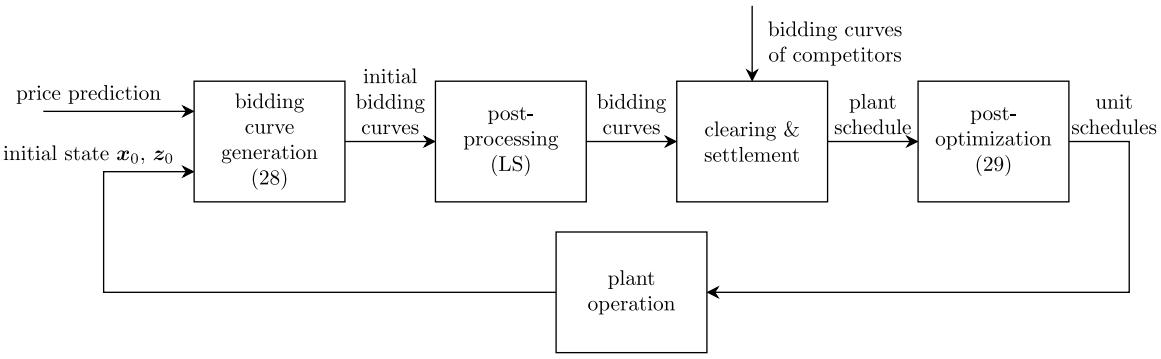

Fig. 11. Overall bidding curve generation strategy.

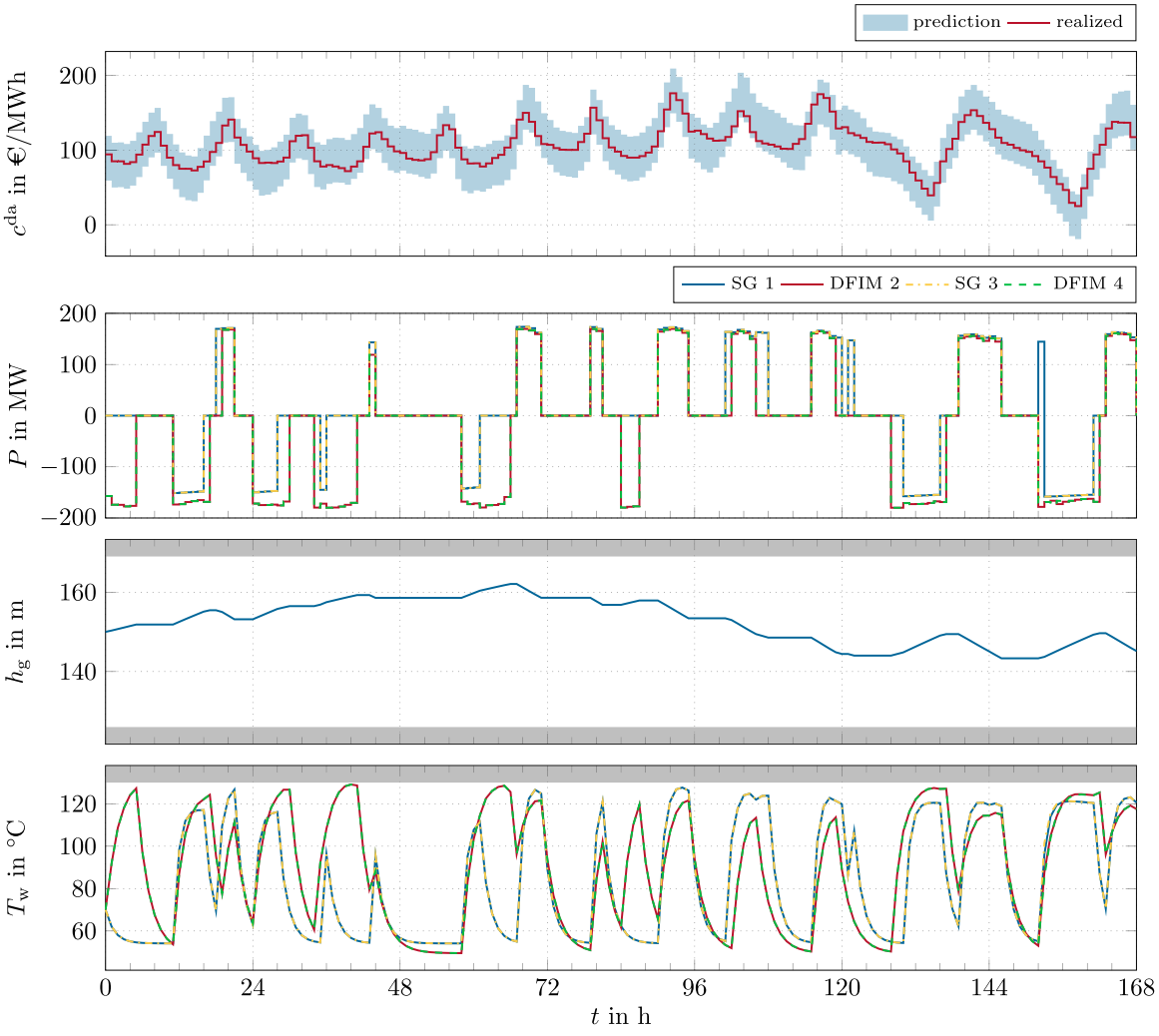

Fig. 12. Operation of a heterogeneous plant consisting of two SGs and two DFIMs with the proposed bidding curve generation strategy for week 24 of 2023 in Austria. The infeasible area is shaded gray.

The developed model was used first to study the optimal operation on the Day-Ahead and ancillary services markets. Based on an a priori known price and a price-taker plant, a mixed integer nonlinear problem (MINLP) was formulated. It was shown that an operation with electrical overload within the permissible thermal limits can increase profit by 16.76 %. The second significant result is a study of the plant profit with different generator types and ancillary services. It is shown that variable-speed generators have higher profits, particularly DFIMs, than fixed-speed SGs. The profit difference is additionally increased if ancillary services are offered, mainly in the case of automatic Frequency Restoration Reserve (aFRR). This comes from the extended flexibility of variable-speed units and the possibility to offer ancillary services in the pump mode operation. The profit of heterogeneous plants lies between the profits of fixed-speed generators and the respective variable-speed technology. It is important to note that detailed characteristics of different generator technologies were used, which allows for a qualitative

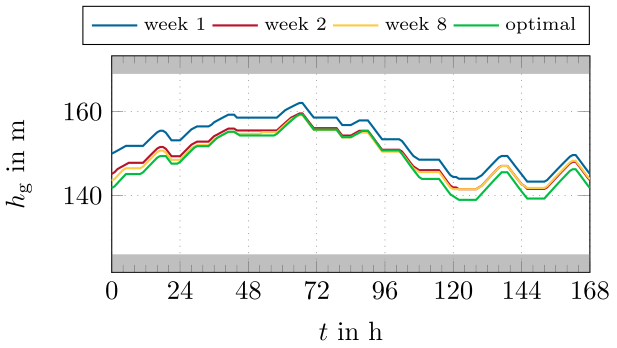

Fig. 13. Gross head during the operation of a plant consisting of two SGs and two DFIMs with the proposed bidding curve generation strategy. The infeasible area is shaded gray.

comparison of different generator types. In contrast, simplified models that do not account for detailed unit characteristics are known from the state of the art, making a direct comparison difficult. The developed MINLP also has low computation times, making the developed model and optimization problem applicable in practice.

The second study was related to the continuous Intraday market, where a MINLP was developed and solved again. It is shown that the increased flexibility of variable-speed units increases profits from trading on the Intraday market. The profit from the Intraday market decreases if the plant offers ancillary services due to the requested reserves. The total profit can decrease if Frequency Containment Reserve (FCR) is offered (with or without aFRR), which is a direct consequence of the lower FCR prices. It might be uneconomical to offer FCR regarding the total profit in the Day-Ahead, ancillary services, and Intraday markets. However, this strongly depends on the market prices.

A strategy for generating PSPP bidding curves based on robust optimization is developed in the last part of this paper. The results show that the proposed bidding curve generation strategy allows the plant to operate with high profits under price prediction uncertainties. The reservoir is also managed optimally as the influence of the gross head on the plant efficiency is considered by the developed model.

The results show that the plant has higher profits for variable-speed than fixed-speed units. The profits for combinations of fixed- and variable-speed units are between the fixed- and the respective variable-speed units. The profits of DFIM-based units are also higher than those of CFSG-based units.

In conclusion, this work shows a significant extension of the studies of optimal operation and bidding curve generation of PSPPs in different markets and under different conditions compared to the state of the art. The proposed model and methods apply to (pumped) storage power plants of various topologies. The first results of the authors showed the applicability to bigger hydropower chains. The main limitation here is the increasing computational time for closely coupled plants, which will be addressed in future work. A suitable price prediction method will also be implemented in future work, and the influence on the bidding curve generation will be studied. Moreover, a price-maker plant will also be studied in this context.

CRediT authorship contribution statement

Domagoj-Krešimir Jukić: Writing – original draft, Visualization, Software, Methodology, Investigation, Formal analysis, Conceptualization. **Andreas Kugi:** Writing – review & editing, Supervision, Project administration, Funding acquisition. **Wolfgang Kemmetmüller:** Writing – review & editing, Supervision, Project administration, Methodology, Funding acquisition, Conceptualization.

Declaration of competing interest

The authors declare the following financial interests/personal relationships which may be considered as potential competing interests: Domagoj-Kresimir Jukic reports financial support was provided by Austrian Research Promotion Agency. Domagoj-Kresimir Jukic reports article publishing charges was provided by TU Wien Library. If there are other authors, they declare that they have no known competing financial interests or personal relationships that could have appeared to influence the work reported in this paper.

Data availability

The data that has been used is confidential.

Acknowledgments

This research was funded by the Austrian Research Promotion Agency (FFG), Austria under grant agreement number 888732. The authors are grateful to the industrial research partner Andritz Hydro GmbH for the provided data and the helpful discussions. In particular, the authors would like to thank Markus Egretzberger, Wolfgang Hofbauer, and Mathias Meusburger for the fruitful discussions.

The authors acknowledge TU Wien Bibliothek for financial support through its Open Access Funding Programme.

References

[1] REN21, Renewables 2022 Global Status Report, Tech. Rep., Paris, France, 2022.

[2] D. Apostolopoulou, M. McCulloch, Optimal short-term operation of a cascaded hydro-solar hybrid system: A case study in Kenya, IEEE Trans. Sustain. Energy 10 (4) (2019) 1878–1889, http://dx.doi.org/10.1109/TSTE.2018.2874810.

[3] F. Najibi, E. Alonso, D. Apostolopoulou, Optimal dispatch of pumped storage hydro cascade under uncertainty, in: 12th UKACC International Conference on Control, Sheffield, United Kingdom, 2018, pp. 187–192, http://dx.doi.org/10.1109/CONTROL.2018.8516823.

[4] J.I. Pérez-Díaz, M. Chazarra, J. García-González, G. Cavazzini, A. Stoppato, Trends and challenges in the operation of pumped-storage hydropower plants, Renew. Sustain. Energy Rev. 44 (2015) 767–784, http://dx.doi.org/10.1016/j.rser.2015.01.029.

[5] M. Chazarra, J.I. Pérez-Díaz, J. García-González, Optimal energy and reserve scheduling of pumped-storage power plants considering hydraulic short-circuit operation, IEEE Trans. Power Syst. 32 (1) (2017) 344–353, http://dx.doi.org/10.1109/TPWRS.2016.2545740.

[6] N. Naval, J.M. Yusta, R. Sánchez, F. Sebastián, Optimal scheduling and management of pumped hydro storage integrated with grid-connected renewable power plants, J. Energy Storage 73 (2023) 108993, http://dx.doi.org/10.1016/j.est.2023.108993.

[7] S. Rehman, L.M. Al-Hadhrami, M.M. Alam, Pumped hydro energy storage system: A technological review, Renew. Sustain. Energy Rev. 44 (2015) 586–598, http://dx.doi.org/10.1016/j.rser.2014.12.040.

[8] X. Ma, D. Wu, D. Wang, B. Huang, K. Desomber, T. Fu, M. Weimar, Optimizing pumped storage hydropower for multiple grid services, J. Energy Storage 51 (2022) 104440, http://dx.doi.org/10.1016/j.est.2022.104440.

[9] S.M. Braun, R. Hoffmann, Intraday optimization of pumped hydro power plants in the german electricity market, in: 5th International Workshop on Hydro Scheduling in Competitive Electricity Markets, Vol. 87, Trondheim, Norway, 2016, pp. 45–52, http://dx.doi.org/10.1016/j.egypro.2015.12.356.

[10] G. Sáenz de Miera, P. del Río González, I. Vizcaíno, Analysing the impact of renewable electricity support schemes on power prices: The case of wind electricity in Spain, Energy Policy 36 (9) (2008) 3345–3359, http://dx.doi.org/10.1016/j.enpol.2008.04.022.

[11] R. Deb, Operating hydroelectric plants and pumped storage units in a competitive environment, Electr. J. 13 (3) (2000) 24–32, http://dx.doi.org/10.1016/S1040-6190(00)00093-2.

[12] J. Pinto, J. de Sousa, M.V. Neves, The value of a pumping-hydro generator in a system with increasing integration of wind power, in: 8th International Conference on the European Energy Market, Zagreb, Croatia, 2011, pp. 306–311, http://dx.doi.org/10.1109/EEM.2011.5953028.

[13] S.M. Braun, C. Brunner, Price sensitivity of hourly day-ahead and quarter-hourly intraday auctions in Germany, Z. Energiewirtschaft 42 (3) (2018) 257–270, http://dx.doi.org/10.1007/s12398-018-0228-0.

[14] S.M. Braun, M. Burkhardt, Trading of pumped storage hydropower plants on energy only and ancillary services markets, in: International Conference on Renewable Energy Research and Applications, Palermo, Italy, 2015, pp. 649–653, http://dx.doi.org/10.1109/ICRERA.2015.7418492.

[15] C. Maier, Investigation of the Dynamic Behavior of Variable Speed Pumped Storage Hydropower Plants for Frequency Containment Reserve Provision (Ph.D. thesis), Technische Universität Wien, Vienna, Austria, 2023, http://dx.doi.org/10.34726/hss.2023.38104.

[16] Swissgrid AG, Prequalification conditions to the respective framework contract for participation in primary, secondary and tertiary regulation, 2022, (in German), https://www.swissgrid.ch/dam/swissgrid/customers/topics/ancillary-services/prequalification/2/Anhang-01-Praequalifikationsbedingungen-de.pdf. (Accessed 24 May 2023).

[17] D.-K. Jukić, A. Kugi, W. Kemmetmüller, Optimal dynamic operation of pumped storage power plants with variable and fixed speed generators, Control Eng. Pract. 138 (2023) 105601, http://dx.doi.org/10.1016/j.conengprac.2023.105601.

[18] T. Key, Quantifying the Value of Hydropower in the Electric Grid: Final Report, Tech. Rep., Energy Efficiency and Renewable Energy, Washington, DC, USA, 2013.

[19] M. Chazarra, J.I. Pérez-Díaz, J. García-González, Optimal operation of variable speed pumped storage hydropower plants participating in secondary regulation reserve markets, in: 11th International Conference on the European Energy Market, Lisbon, Portugal, 2014, pp. 1–5, http://dx.doi.org/10.1109/EEM.2014.6861264.

[20] M. Chazarra, J.I. Pérez-Díaz, J. García-González, Optimal joint energy and secondary regulation reserve hourly scheduling of variable speed pumped storage hydropower plants, IEEE Trans. Power Syst. 33 (1) (2018) 103–115, http://dx.doi.org/10.1109/TPWRS.2017.2699920.

[21] J. Schmidt, W. Kemmetmüller, A. Kugi, Modeling and static optimization of a variable speed pumped storage power plant, Renew. Energy 111 (2017) 38–51, http://dx.doi.org/10.1016/j.renene.2017.03.055.

[22] J.-F. Mennemann, L. Marko, J. Schmidt, W. Kemmetmüller, A. Kugi, Nonlinear model predictive control of a variable-speed pumped-storage power plant, IEEE Trans. Control Syst. Technol. 29 (2) (2021) 645–660, http://dx.doi.org/10.1109/TCST.2019.2956910.

[23] J.I. Pérez-Díaz, J.R. Wilhelmi, J.Á. Sánchez-Fernández, Short-term operation scheduling of a hydropower plant in the day-ahead electricity market, Electr. Power Syst. Res. 80 (12) (2010) 1535–1542, http://dx.doi.org/10.1016/j.epsr.2010.06.017.

[24] J. Kwon, T. Levin, V. Koritarov, Optimal market participation of pumped storage hydropower plants considering hydraulic short-circuit operation, in: 52nd North American Power Symposium, Tempe, AZ, USA, 2020, pp. 1–6, http://dx.doi.org/10.1109/NAPS50074.2021.9449644.

[25] H. Alharbi, K. Bhattacharya, Participation of pumped hydro storage in energy and performance-based regulation markets, IEEE Trans. Power Syst. 35 (6) (2020) 4307–4323, http://dx.doi.org/10.1109/TPWRS.2020.2998490.

[26] A. Conejo, J. Arroyo, J. Contreras, F. Villamor, Self-scheduling of a hydro producer in a pool-based electricity market, IEEE Trans. Power Syst. 17 (4) (2002) 1265–1272, http://dx.doi.org/10.1109/TPWRS.2002.804951.

[27] S. Tian, J. He, Y. Xin, F. Xu, Z. Wang, Q. Hao, Research on day-ahead optimal dispatch considering the mutual constraint of pumped storage unit, in: International Conference on Intelligent Computing, Automation and Systems, Chongqing, China, 2020, pp. 255–260, http://dx.doi.org/10.1109/ICICAS51530.2020.00059.

[28] R. Baldick, Y. Chen, B. Huang, Optimization formulations for storage devices with disjoint operating modes, Oper. Res. 71 (6) (2023) 1978–1996, http://dx.doi.org/10.1287/opre.2023.2482.

[29] S.J.P.S. Mariano, J.P.S. Catalão, V.M.F. Mendes, L.A.F.M. Ferreira, Profit-based short-term hydro scheduling considering head-dependent power generation, in: IEEE Lausanne Power Tech, Lausanne, Switzerland, 2007, pp. 1362–1367, http://dx.doi.org/10.1109/PCT.2007.4538514.

[30] J.P.S. Catalão, S.J.P.S. Mariano, V.M.F. Mendes, L.A.F.M. Ferreira, Nonlinear approach for short-term scheduling of a head-sensitive hydro chain, in: IEEE Russia Power Tech, Saint Petersburg, Russia, 2005, pp. 1–6, http://dx.doi.org/10.1109/PTC.2005.4524346.

[31] J.P.S. Catalão, S.J.P.S. Mariano, V.M.F. Mendes, L.A.F.M. Ferreira, Scheduling of head-sensitive cascaded hydro systems: A nonlinear approach, IEEE Trans. Power Syst. 24 (1) (2009) 337–346, http://dx.doi.org/10.1109/TPWRS.2008.2005708.

[32] M. Olsson, L. Söder, Hydropower planning including trade-off between energy and reserve markets, in: IEEE Bologna Power Tech, Bologna, Italy, 2003, p. 8, http://dx.doi.org/10.1109/PTC.2003.1304117.

[33] B. Flamm, A. Eichler, J. Warrington, J. Lygeros, Two-Stage Dual Dynamic Programming With Application to Nonlinear Hydro Scheduling, IEEE Trans. Control Syst. Technol. 29 (1) (2021) 96–107, http://dx.doi.org/10.1109/TCST.2019.2961645.

[34] P. Toufani, E.C. Karakoyun, E. Nadar, O.B. Fosso, A.S. Kocaman, Optimization of pumped hydro energy storage systems under uncertainty: A review, J. Energy Storage 73 (2023) 109306, http://dx.doi.org/10.1016/j.est.2023.109306.

[35] S. Shafiee, H. Zareipour, A.M. Knight, Developing bidding and offering curves of a price-maker energy storage facility based on robust optimization, IEEE Trans. Smart Grid 10 (1) (2019) 650–660, http://dx.doi.org/10.1109/TSG.2017.2749437.

[36] R. Weron, Electricity price forecasting: A review of the state-of-the-art with a look into the future, Int. J. Forecast. 30 (4) (2014) 1030–1081, http://dx.doi.org/10.1016/j.ijforecast.2014.08.008.

[37] L. Baringo, A.J. Conejo, Offering Strategy Via Robust Optimization, IEEE Trans. Power Syst. 26 (3) (2011) 1418–1425, http://dx.doi.org/10.1109/TPWRS.2010.2092793.

[38] Q.P. Zheng, J. Wang, A.L. Liu, Stochastic optimization for unit commitment – A review, IEEE Trans. Power Syst. 30 (4) (2015) 1913–1924, http://dx.doi.org/10.1109/TPWRS.2014.2355204.

[39] J. García-González, R.M.R. de la Muela, L.M. Santos, A.M. González, Stochastic Joint Optimization of Wind Generation and Pumped-Storage Units in an Electricity Market, IEEE Trans. Power Syst. 23 (2) (2008) 460–468, http://dx.doi.org/10.1109/TPWRS.2008.919430.

[40] A.J. Conejo, F. Nogales, J.M. Arroyo, Price-taker bidding strategy under price uncertainty, IEEE Trans. Power Syst. 17 (4) (2002) 1081–1088, http://dx.doi.org/10.1109/TPWRS.2002.804948.

[41] D.-K. Jukić, A. Kugi, W. Kemmetmüller, Optimal guide vane closing schemes for pumped storage power plants, IEEE Trans. Control Syst. Technol. 31 (4) (2023) 1537–1551, http://dx.doi.org/10.1109/TCST.2022.3225743.

[42] D. Staton, E. Chong, S. Pickering, A. Boglietti, Cooling of Rotating Electrical Machines: Fundamentals, Modelling, Testing and Design, The Institution of Engineering and Technology, London, United Kingdom, 2022.

[43] C. Trivedi, B. Gandhi, C.J. Michel, Effect of transients on Francis turbine runner life: a review, J. Hydraul. Res. 51 (2) (2013) 121–132, http://dx.doi.org/10.1080/00221686.2012.732971.

[44] R. Fisher, J. Koutník, L. Meier, V. Loose, K. Engels, T. Beyer, A comparison of advanced pumped storage equipment drivers in the US and Europe, in: HydroVision, Louisville, KY, USA, 2012, pp. 1–30, http://dx.doi.org/10.13140/2.1.1082.4967.

[45] P.M. Pfeifroth, Modeling the Deployment Planning of Functional Electricity Storage for Electricity and Balancing Power Markets (Ph.D. thesis), Technische Universität München, Munich, Germany, 2015 (in German).

[46] A. Peiravi, D. Thibault, M. Blain, M. Nourelfath, M.K. Zanjani, Start/stop cost evaluation of a francis turbine runner based on reliability, in: 16th World Congress on Engineering Asset Management, Seville, Spain, 2023, pp. 261–269, http://dx.doi.org/10.1007/978-3-031-25448-2_25.

[47] J.A.E. Andersson, J. Gillis, G. Horn, J.B. Rawlings, M. Diehl, CasADi – A software framework for nonlinear optimization and optimal control, Math. Program. Comput. 11 (1) (2019) 1–36, http://dx.doi.org/10.1007/s12532-018-0139-4.

[48] I. Quesada, I.E. Grossmann, An LP/NLP based branch and bound algorithm for convex MINLP optimization problems, Comput. Chem. Eng. 16 (10) (1992) 937–947, http://dx.doi.org/10.1016/0098-1354(92)80028-8.

[49] R.H. Byrd, J. Nocedal, R.A. Waltz, Knitro: An Integrated Package for Nonlinear Optimization, Springer, Boston, MA, USA, 2006, pp. 35–59, http://dx.doi.org/10.1007/0-387-30065-1_4.